arXiv:1403.3059v1 [cond-mat.mtrl-sci] 12 Mar 2014

Study of van der Waals bonding and interactions in metal organic framework materials

Sebastian Zuluaga

Department of Physics, Wake Forest University, Winston-Salem, NC 27109, USA.

Pieremanuele Canepa

Department of Physics, Wake Forest University, Winston-Salem, NC 27109, USA.

Kui Tan

Department of Materials Science and Engineering, University of Texas at Dallas, TX 75080, USA.

Yves J. Chabal

Department of Materials Science and Engineering, University of Texas at Dallas, TX 75080, USA.

Timo Thonhauser

E-mail: thonhauser@wfu.edu
Department of Physics, Wake Forest University, Winston-Salem, NC 27109, USA.

Abstract. Metal organic framework (MOF) materials have attracted a lot of attention due to their numerous applications in fields such as hydrogen storage, carbon capture, and gas sequestration. In all these applications, van der Waals forces dominate the interaction between the small guest molecules and the walls of the MOFs. In this review article, we describe how a combined theoretical and experimental approach can successfully be used to study those weak interactions and elucidate the adsorption mechanisms important for various applications. On the theory side, we show that, while standard density functional theory is not capable of correctly describing van der Waals interactions, functionals especially designed to include van der Waals forces exist, yielding results in remarkable agreement with experiment. From the experimental point of view, we show examples in which IR adsorption and Raman spectroscopy are essential to study molecule/MOF interactions. Importantly, we emphasize throughout this review that a combination of theory and experiment is crucial to effectively gain further understanding. In particular, we review such combined studies for the adsorption mechanism of small molecules in MOFs, the chemical stability of MOFs under humid conditions, water cluster formation inside MOFs, and the diffusion of small molecules into MOFs. The understanding of these phenomena is critical for the rational design of new MOFs with desired properties.

1. Introduction

Metal organic framework (MOF) materials are nano-porous materials comprised of metal centers, which are linked by organic ligands. Over the past decade, MOFs have attracted a surge of attention due to their extraordinary properties, useful for hydrogen storage [1–4], CO_2 capture [5–9], catalysis [10–12], and sensing [13] among others [14, 15]. Part of the success of MOFs also has to do with their often simple synthesis, i.e. by combining the organic ligands and the metallic salt in a solvothermal reaction [16, 17]. Most practical applications of MOFs rely on a specific interaction of the MOF with small molecules. This interaction—typically of a weak van der Waals type—has thus been at the center of many experimental and theoretical studies. It is exactly the understanding of this interaction that will allow us to interpret the properties of current MOFs better and design new and improved MOFs with desired properties. For example, we do know that, in general, the MOFs surface area and the binding strength to the metal centers are the two main factors controlling the uptake of small molecules. However, the exact correlation between those properties is unclear [18]. Another example concerns much current research, trying to address the problem of low stability of MOFs under humid conditions. While some progress has been made [19–24], the newly found water-resistant MOFs often lack the desired specific molecular uptakes that are needed. Overall, progress has been slow to address such questions due to a lack of appropriate methods to study the molecular interactions inside MOFs. In the present review article we highlight a strategy, combining experiment and theory, that overcomes these problems and has been particularly successful in unraveling van der Waals interactions in MOFs.

The experimental study of those interactions often relies on powerful vibrational spectroscopy such as infrared (IR) absorption and Raman scattering, which indirectly provide information about the molecular adsorption process taking place in the MOF. The theoretical description with *ab initio* methods, due to the typical size of MOF unit cells and their extended nature, rules out most highly accurate quantum-chemistry approaches and leaves density functional theory (DFT) as the only viable option. Historically, however, standard exchange-correlation functionals within DFT such as LDA and GGA only poorly capture van der Waals interactions. We will show here that the specially designed functional vdW-DF [25–27] is in fact capable to describe van der Waals interactions reliably and gives results in remarkable agreement with experiment.

This review article aims to showcase the importance of IR and Raman spectroscopy techniques combined with *ab initio* simulations at the DFT level (utilizing vdW-DF) as a promising way to study and rationally design complex systems where van der Waals bonding plays a major role. To this end, this work is divided into several sections. In Section 2, we give a description of the success and failures of vibrational spectroscopic techniques to study van der Waals interactions. Then, in Section 3, we present a description of the computer simulations used to describe and interpret complex spectroscopic experiments. In Section 4, we present several relevant examples where the

combination of experiment and theory explains the behavior of various MOF systems and provides much needed understanding. We conclude with a short summary and outlook in Section 5.

2. Success and Failure of Vibrational Spectroscopies to study van der Waals Interactions

2.1. IR and Raman spectroscopy of small molecule adsorption in MOFs

IR and Raman spectroscopy provide complementary information about bonding configurations through their vibrational spectra. IR spectra reflect photon absorption during transitions from ground- to first-excited vibrational levels ($\nu = 0 \rightarrow 1$) in the electronic ground state, requiring a dynamic dipole moment (associated with a change in the dipole moment during the vibrational motion) [28]. In contrast, Raman spectroscopy is based on photon scattering by molecules and has its origin in the electronic polarization caused by monochromatic visible radiation [28, 29]. Therefore, a vibrational mode is Raman active if the polarizability is modulated during the vibration [28,29]. Strict selection rules exist for both spectroscopies, sometimes leading to complementary detection [29]. For example, the vibration of the homopolar diatomic molecule H_2 is not IR active (due to the absence of a fluctuating dipole associated with the symmetric stretching), but strongly Raman active. However, once the molecule interacts with the MOF, it undergoes a perturbation that slightly polarized the originally symmetric molecule and makes it weakly IR active. This perturbation is usually accompanied by a red-shift of the H–H stretching modes, located at 4161.1 cm^{-1} and 4155 cm^{-1} for para and ortho H_2, respectively [30]. For the linear molecule CO_2, the symmetric stretch mode (ν_1) is Raman active but not IR active, whereas the antisymmetric modes (ν_2 and ν_3) are IR active [29].

Based on these principles, IR and Raman spectroscopy can be very useful tools to characterize the nature of host/guest interactions [31–34] in MOFs. Particularly valuable information can be gained by identifying perturbations of the IR active modes. For example, the first spectroscopic evidence for the formation of an electron-donor acceptor (EDA) complex between CO_2 and functional groups of MOFs was observed in a MOF of type MIL–53 and reported in later studies of adsorption of CO_2 in amino-based MOFs [32,33]. The adsorption of CO_2 molecules in MIL–53 leads to a modest red-shift from -10 cm^{-1} to -15 cm^{-1} of the stretching mode ν_3 and to a splitting of the bending mode ν_2 due to the removal of degeneracy of the in-plane and out-of-plane bends [32]. A similar splitting of ν_2 modes is common in many electron-donor acceptor complexes of CO_2 with organic solvents or polymers possessing electron-donating functional groups—e.g., carbonyl groups—due to the interaction of the carbon atom of CO_2 as the electron acceptor [35,36]. Moreover, significant perturbations of both ν(OH) and σ(OH) bands of hydroxyl groups (ν(OH) = 19 cm^{-1} and σ(OH) = 30 cm^{-1}) suggest that oxygen atoms of the framework hydroxyl group act as the electron donor [32].

As evident from these examples (and many others), it is clear that IR and Raman spectroscopy, by themselves and even without the aid of theoretical calculations, can often provide insight into the interactions between guest molecules and the MOF. However, as we will see in the next section, in other cases the "blind" application of these spectroscopic techniques can lead to a significant misinterpretation of the experimental data obtained. This can happen when IR and Raman spectroscopy are used as *indirect* probes—i.e. deducing other physical properties of the system from a simple red- or blue-shift in the spectrum. In such cases, theory and computer simulations are essential to derive a complete understanding, as they provide *direct* access to many properties of the system, and often provide interpretations that are unexpected from simple correlations in the experimental data.

2.2. Difficulty of IR and Raman spectroscopy to describe small molecule adsorption in MOFs

Despite the high sensitivity of spectroscopy to molecular interactions with the MOF, attention must be paid when interpreting the data to extract information about the interaction from vibrational frequency shifts, intensities, and line-widths [37, 38]. For example, it is commonly accepted that the magnitude of the IR shift of small adsorbed molecules in MOFs is directly related to their adsorption energy, and thus the IR shift can be used indirectly to estimate the relative adsorption energies. However, in our recent IR spectroscopy study of molecular hydrogen in a number of different MOF compounds [37] , we find that there is no clear correlation between H_2 adsorption energies (determined by isotherm measurements) and the magnitude of the H_2 stretch shift. In fact, metal-formate $M_3(HCOO)_6$ [M = Co, Ni and Mn] compounds with the highest adsorption energy have the lowest hydrogen IR shift. In this case, we find that the IR shift is dominated by the environment (organic ligand, metal center, and structure) [37], rather than by the adsorption energy to the metal.

Similarly, integrated areas for the specific IR bands were long considered to be directly correlated with the amount (loading) of adsorbed molecules, assuming that the dipole moment of the adsorbed species is not affected by loading or site geometry [39–41]. Based on this assumption, variable temperature IR was used to measure the absorbance of IR bands (including that of H_2 molecules) and estimate the adsorption energy [39,41]. However, our theoretical and experimental findings for H_2 molecules in MOF74 with unsaturated metal centers indicate that large variations in the induced dipole moment take place as a function of loading, due to the interaction among adsorbed molecules [38]. In the case of Mg-MOF74, the effective charge of H_2 at the metal sites weakens (from 0.021 e to 0.015 e as the loading increases from 1 to 12 H_2/primitive cell) i.e. as the neighboring sites are occupied. Thus, the IR intensity is reduced by 50%, since it is proportional to the square of the effective charge or the dynamic dipole moment [38]. These findings suggest that the integrated areas of IR bands do not always correlate with the amount of H_2 adsorbed and possible variations in dynamic dipole moments

have to be taken into account.

In summary, IR and Raman spectroscopy can be very helpful tools when studying small molecule adsorption in MOFs. But, extreme caution is necessary when utilizing those methods to make assumptions about adsorption energies or loadings, as illustrated in the examples given above. Under these circumstances, theoretical input using first principles calculations—specifically capable to deal with van der Waals interactions—is critical to interpret experimental observations correctly.

2.3. Experimentation

Zecchina and coworkers first used transmission IR spectroscopy to study the fundamental aspects of the interaction between H_2 and MOFs, mainly in the low temperature (<300 K) and pressure regime. By means of the variable temperature infrared (VTIR) spectroscopy method, the adsorption enthalpy was derived by measuring the intensity of absorption bands as a function of temperature [40, 42]. However, caution must be taken when using the VTIR method since the dipole moment might change as a function of loading, as pointed out above. More recent work [24, 37, 38, 43] has investigated a series of small molecules (H_2, CO_2, CH_4, SO_2, H_2O, etc.) using *in situ* IR absorption spectroscopic to quantify the effect of their interaction with different types of MOFs in a wide range of pressures (from 50 mTorr to 55 bar) and temperatures (10 K to 423 K). In order to perform the IR measurements at and above room temperature, a portion (∼10 mg) of MOF was lightly pressed onto a KBr support and mounted into a high-temperature high-pressure cell (Specac product number P/N 5850c) and further heated in vacuum for activation. During the annealing, the removal of solvent molecules was monitored by *in situ* IR spectroscopy. Then, the activated sample was cooled to specific temperatures in order to perform the measurements at specific pressure gas exposures. Measurements were performed in transmission using a liquid–N_2 cooled InSb/MCT detector. Similar measurements were also performed in a Janis PTSHI series cold refrigerator (CCR) system for low temperature studies (<298 K). In addition to transmission IR, diffuse reflectance infrared Fourier transform spectroscopy (DRIFTS) was employed to investigate the dynamics of H_2 molecules adsorbed within the MOF74 compounds [33, 34]. Furthermore, DRIFTS has also been used to study the interactions between CO_2 and functional groups on the organic ligands of some MOFs under the controlled *in situ* cell environment [44–46].

Most recently, *in situ* Raman spectroscopy was also used to study the structural response mechanism of flexible metal organic frameworks $Zn_2(bpdc)_2bpee$ [bpdc = 4,40-biphenyl dicarbox-ylate and bpee = 1,2-bis(4-pyridyl)ethylene] upon CO_2, N_2, and hydrocarbon molecules adsorption [47, 48]. In this case, Raman spectroscopy is more suitable because the phonon modes of the MOFs do not overwhelm the spectra as they do in the case of IR spectra, which include a large number of combination and overtone bands. By integrating a Linkam FTIR600 cooling/heating stage, the activated sample was measured under the controlled temperature and gas environment. The changes on

specific bonds in the MOF structure, monitored by Raman spectroscopy, were correlated to the MOF structural changes and the guest-host interactions.

3. Computer Simulations as a Tool to Interpret Complex Spectroscopic Experiments

3.1. Ab initio modeling of materials

While very successful classical modeling techniques exist, such as force field simulations, which are suitable for studying very large systems, they are not capable of describing the electronic structure of materials and the intricate role it plays in many processes. In the case of MOF materials, we are most interested in electronic-structure changes during the adsorption and desorption of small molecules in their cavities, as well as a number of catalytic processes. As such, unless cost prohibitive, *ab initio* modeling techniques are the methods of choice. For an overview of widely-used materials-modeling techniques, ranging from classical approaches to high-level quantum-chemistry methods, see Ref. [49].

Modeling MOF materials with *ab initio* methods presents a particular challenge. The adsorption/desorption of small molecules in MOFs is often governed by physisorption, i.e. weak van der Waals forces, which are difficult to capture correctly with *ab initio* methods. Correlated high-level quantum-chemistry approaches, such as Møller-Plesset perturbation theory and coupled-cluster methods [50], can describe van der Waals interactions, but their computational cost limits them to small systems ($\sim$100 and $\sim$30 atoms, respectively [51]) and their application to large periodic systems, such as the MOFs of interest here, is unpractical [52–57].

Density functional theory (DFT) [58], on the other hand, has a much more favorable computational cost and can be used for systems with up to 1000 atoms—in linear-scaling DFT even up to 1,000,000 atoms [51]. It is also easily implemented with periodic plane-wave basis sets, such that treating periodic systems becomes trivial. Unfortunately, with standard exchange-correlation functionals, DFT cannot reliably describe van der Waals interactions [59–62], a phenomenon where charge fluctuations in one part of the system correlate with fluctuations in another, resulting in an attractive force that is a *truly nonlocal correlation effect* [63]. It follows that standard local and semi-local functionals, such as LDA and GGA, cannot reliably account for these nonlocal effects and yield qualitatively erroneous predictions [64–67]. While very promising extensions exist [64], most notably DFT-D [68, 69], DFT-SAPT [70–72], and C_6-based methods [73, 74], they are semi-empirical, perturbative, and not seamlessly self-consistent density functionals.

3.2. vdW-DF: a good compromise between cost and accuracy

We have overcome this problem and include van der Waals forces self-consistently in DFT [26] in the form of a van der Waals density functional (vdW-DF). Its accuracy is comparable to high-level quantum-chemistry approaches [75–77]. vdW-DF goes beyond

standard DFT to include a *truly nonlocal correlation* $E_c^{\rm nl}$ in the exchange-correlation energy E_{xc},

$$E_{xc}[n] = E_x^{\rm revPBE}[n] + E_c^{\rm LDA}[n] + E_c^{\rm nl}[n] \ , \tag{1}$$

$$E_c^{\rm nl}[n] = \frac{1}{2}\int d^3r\, d^3r'\ n(\vec{r})\phi(\vec{r},\vec{r}')n(\vec{r}') \ , \tag{2}$$

where n is the electron density and revPBE [78] and LDA [79] are standard functionals. $E_c^{\rm nl}$ is determined by the kernel ϕ, which is a complicated function of the densities and their gradients at $\vec{r}$ and $\vec{r}'$, first developed by Langreth et al. [25]. With the corresponding exchange-correlation potential $v_c^{\rm nl}(\vec{r}) = \delta E_c^{\rm nl}[n]/\delta n(\vec{r})$ [26], the method becomes self-consistent and permits calculation of atomic forces—essential for structural optimization and molecular-dynamics simulations. Like high-level quantum-chemical methods, vdW-DF precludes bias through a full, self-consistent solution of the coupled Schrödinger equations for all valence electrons. Calculations automatically include direct and induced electrostatic effects, charge transfer effects, and effects due to the non-nuclear centricity of the dispersion interaction as well as its deviations from the inverse sixth power at smaller than asymptotic separations.

vdW-DF can be implemented in standard plane-wave electronic-structure codes exploiting an efficient Fast Fourier Transform algorithm [80]. This algorithm scales like standard DFT, and for large systems compute times are negligibly longer than for GGA calculations. We routinely use our own implementation to study hydrogen-storage materials with 300 to 400 atoms per unit cell [81,82]. In particular, we have successfully used vdW-DF to study a variety of phenomena in MOF materials, achieving remarkable agreement with experiment [24, 43, 48, 83–90].

3.3. Comparison between vdW-DF simulations and experiment

In MOF adsorption studies, there are ample opportunities for theory and experiment to interact. It is almost straight forward to compare vdW-DF optimized structures with diffraction experiments [91–93]. Of more interest is the comparison of calculated adsorption energies with measured heats of adsorption [94–98]. As pointed out above, IR spectroscopy can be a very powerful method to study the loading of MOFs, but caution is neccesary. From the theoretical side, while the full calculation of IR spectra is possible [99], it is much easier and typically sufficient to calculate the IR peak positions—this has been done in a number of studies and shows very good agreement with experiment [83, 85, 97]. Comparison with IR experiments has also been made for vdW-DF calculations of small molecule diffusion [86]. vdW-DF calculations for an exhaustive list of elastic and transport properties of MOFs are also compared with experiment [92, 100, 101].

Table 1. Vibrational frequencies (cm^{-1}) of CO_2 physiadsorbed in MOF74. Data taken from Ref. [83].

	System	Bending mode (ν_2)	Asym. stretch mode (ν_3)
exp.	Free CO_2	667	2349
	Mg-MOF74	658	2352
	Zn-MOF74	658	2338
calc.	Free CO_2	646.6	2288.5
	Mg-MOF74	636.6	2288.0
	Zn-MOF74	637.6	2280.4

4. Examples of Successful Combined Experimental/Theoretical studies

4.1. Studying adsorption mechanisms of small molecules in MOFs

It has been shown that MOFs with unsaturated metal centers, such as MOF74 and HKUST-1, exhibit a fast and specific CO_2 absorption, which is a desirable property for capturing applications [47, 102–104]. Therefore, understanding their absorption mechanisms is critical for the rational design of improved MOFs. In this subsection we discuss and analyze the CO_2 absorption in MOF74. We will show that the vdW-DF approach is critical in order to understand and correctly explain the corresponding experimental results. As an example, we review the CO_2 absorption in Zn-MOF74 and Mg-MOF74 and show how the frequency of the asymmetric and stretching modes are modified upon absorption [83].

The experimental IR absorption spectra results in Figure 1 show that the unperturbed asymmetric stretch mode of CO_2 (2349 cm^{-1}) undergoes a shift of -11 cm^{-1} and $+3$ cm^{-1} upon adsorption on Zn-MOF74 and Mg-MOF74, respectively. But, what causes this shift? To answer this question, *ab initio* calculations were performed utilizing vdW-DF, finding three factors contributing to this shift, i.e. (i) the change in the CO_2 molecule length, (ii) the asymmetric distortion of the CO_2 molecule, and (iii) the direct influence of the metal center.

In Table 1, we compare the IR spectroscopy data with results from frozen-phonon vdW-DF calculations, where the CO_2 molecule was adsorbed at the metal site of MOF74. In particular, the frozen-phonon calculations for the bending mode of CO_2 give a change in frequency of approximately -9 cm^{-1} during adsorption on either metal, in excellent agreement with the experimental results. Furthermore, the calculations show that the asymmetric stretch mode of the CO_2 molecule exhibits a red-shift of -0.5 cm^{-1} and -8.1 cm^{-1} when adsorbed on Mg-MOF74 and Zn-MOF74, respectively, in reasonable agreement with the change of $+3$ cm^{-1} and -11 cm^{-1} measured in experiment.

According to vdW-DF calculations [83], the CO_2 molecule binds stronger to Mg-MOF74 than to Zn-MOF74, in agreement with experimental findings. Furthermore, the distance between the metal center and the CO_2 molecule is smaller in Mg-MOF74 than in Zn-MOF74. Also, the CO_2 molecule experiences a larger distortion upon adsorption

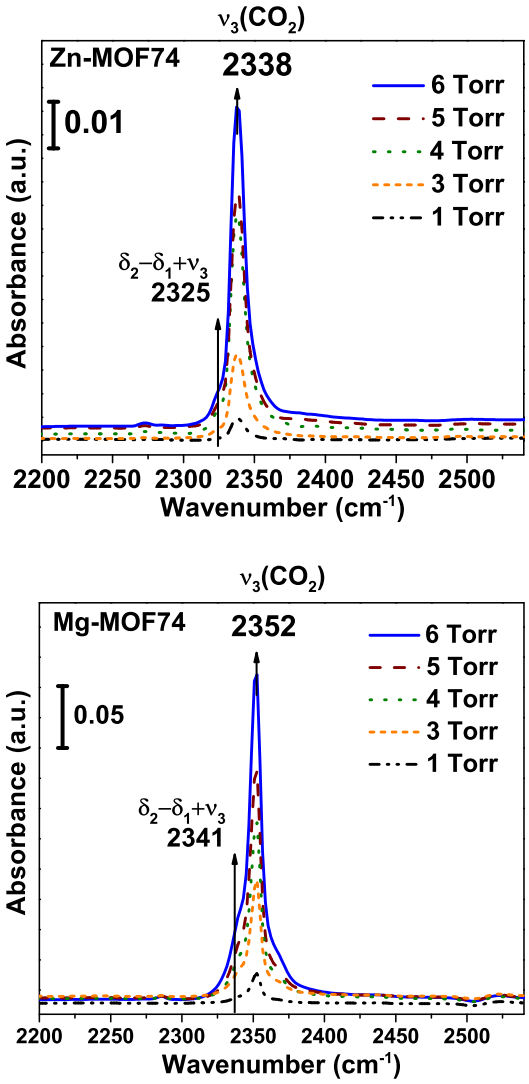

Figure 1. IR absorption spectra of CO_2 absorbed into Zn-MOF74 (top) and in Mg-MOF74 (bottom) at changing CO_2 pressure (1−6 Torr). (Reprinted with permission from Ref. [83]. © 2012 American Physical Society).

in Mg-MOF74, see Table 1 in Ref. [83]. Therefore, it is surprising that the frequency shift of the asymmetric stretching mode (see ν_3 in Table 1) for CO_2 in Mg-MOF74 is smaller compared with that in Zn-MOF74, and a deeper investigation of what causes this peculiar result is warranted. As mentioned above, this result can be explained with the help of theory.

We will start with the change in the molecule length: in order to analyze this effect, phonon calculations of the free CO_2 molecule were performed, where its length was set to the value when adsorbed in the MOF, keeping the carbon atom centered. Using this approach, frequency shifts of -1.6 cm^{-1} and -3.7 cm^{-1} were obtained for the case of Mg- and Zn-MOF74, respectively. It is interesting to see that in the case of Mg-MOF74, the molecule experiences a marginal elongation of 0.0003 Å, while in the case of Zn-MOF74 an elongation of 0.0009 Å takes place. That is, the molecule that

experiences the larger elongation, exhibits the larger red-shift, as suggested by common sense.

The effect corresponding to the molecule's asymmetric distortion was studied by placing the CO_2 molecule exactly at the same geometry as when adsorbed in the MOF, but removing the surrounding MOF. By doing this, the only contributions to the change in frequency come from the elongation of the CO_2 molecule and the asymmetric distortion of the carbon atom. The former has been reported in the paragraph above, so that the latter can easily be calculated. In this way, we find the shift corresponding to the induced asymmetry of the CO_2 molecule to be 1.1 cm^{-1} and 0.7 cm^{-1} for Mg-MOF74 and Zn-MOF74, respectively.

Finally, the effect of the metal center was studied by placing the free, undistorted CO_2 molecule at the metal adsorption site with the same position and angle of the adsorbed system. By doing this, the change in frequency has its highest contribution coming from the oxygen–metal interaction. Using this configuration, the results show a frequency shift of the asymmetric stretching mode of the CO_2 molecule of -5 cm^{-1} for the Zn-MOF74 system. On the other hand, for the Mg-MOF74 the frequency shift has a negligible value of -0.6 cm^{-1}. This is a striking result, since Mg and Zn have a very similar valence structure with $3s$ and $4s$ electrons as the outermost valence states. This result shows that the fully occupied semi-core $3d$ electrons in Zn have an important effect on the interaction with the adsorbed CO_2 molecules. Similar results are found in Co- and Ni-MOF74 structures. To shed more light on this situation, a charge-density analysis was performed, finding a depletion of electrons around the Zn atom upon adsorption of the CO_2 molecule, while this depletion was not present for Mg-MOF74. Thus, the depletion of charge is an effect of the Zn d orbitals, which, in turn, also influences the charge distribution in the adsorbed CO_2 molecule. Via this mechanism, the Zn d orbitals indirectly affect the IR frequency shift of the adsorbed CO_2 molecule—explaining the differences between Mg-MOF74 and Zn-MOF74.

In summary, this van der Waals study of small molecule adsorption on MOFs is driven by experimental IR data. But, it is clear that the reasons for the observed IR frequency shifts are not necessarily intuitive and can only be explained with the help of detailed first-principles simulations.

4.2. Studying the chemical stability of MOFs under humid conditions

The stability of MOFs under humid conditions [105–110] is of great importance for the implementation of these systems in various applications and devices. For example, the MOF5 structure is very sensitive to water and its hydrogen uptake properties become compromised when it is exposed to humidity in ambient air. So, how can we design new MOFs that keep their desired properties while being water resistant? In the case of MOF5, Yeng et al. [105] reported the synthesis of methyl- and 2,5-dimethyl-modified versions. By introducing methyl into the linkers, the structure becomes less reactive to water and retains the same hydrogen uptake properties of MOF5 up to 4 days after being

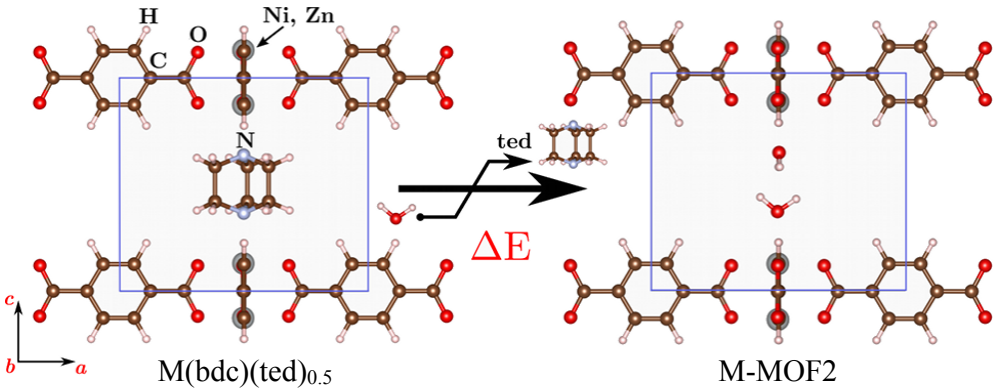

Figure 2. Scheme adopted for water insertion in $M(bdc)(ted)_{0.5}$ [M = Zn, Ni], where the ted group has been substituted by two water molecules. (Reprinted with permission from Ref. [43]. © 2012 American Chemical Society).

exposed to ambient air. While this is a specific case, resting on the specific interaction of water and H_2 with the methyl-modified linkers, it can easily be generalized and it is again the interaction of small molecules—in this case water—with the MOF that is the focus of much ongoing research.

In this subsection, we review efforts to understand the MOF–water interaction, using as an example the prototypical metal organic framework $M(bdc)(ted)_{0.5}$ [M = Cu, Zn, Ni, Co; bdc = 1,4-benzenedicarboxylate; ted = triethylenediamine]. This MOF has shown promising properties towards the adsorption of gases, such as H_2, CO_2, and CH_4 [111–113]. $M(bdc)(ted)_{0.5}$ exhibits thermal stability up to 282°C, is highly porous, the H_2 adsorption is exceptionally high, and it can also adsorb a large amount of hydrocarbons. This system was first synthesized and reported by Dybtsev et al. in Ref. [113] and we will review here its water stability, as originally studied in Ref. [43]. A characteristic building block of this particular MOF is the incorporated "paddle wheel" building-block ted (triethylenediamine), which acts as a linker. In the presence of water, this paddle wheel structure can be extracted from the framework and be replaced by water molecules, forming M-MOF2 (we will refer to it as MOF2), as can be seen in Figure 2. Obviously, with its normal linker missing, the $M(bdc)(ted)_{0.5}$ structure looses stability and, in most cases, undergoes an non-reversible phase transition.

Figure 3 shows the powder X-ray diffraction (XRD) pattern of four hydrated $M(bdc)(ted)_{0.5}$ systems [M = Cu, Zn, Co, and Ni] after exposure to 9.5 Torr of D_2O vapor and the corresponding activated (pristine) $M(bdc)(ted)_{0.5}$ samples. Concerning the $Cu(bdc)(ted)_{0.5}$ system, the XRD pattern confirms that the system is stable after exposure to D_2O gas up to a pressure of 6 Torr, see Figure S10 in the supporting information of Ref. [43]. However, the top left panel of Figure 3 shows that all the X-ray peaks are shifted to higher angles, except for the [001] peak, indicating that the $Cu(bdc)(ted)_{0.5}$ system is partially hydrolyzed by the D_2O molecules. Even though the structure is only partially hydrolyzed, the original $Cu(bdc)(ted)_{0.5}$ structure cannot be recovered after evacuation of water at a temperature of 150°C. In contrast, the left

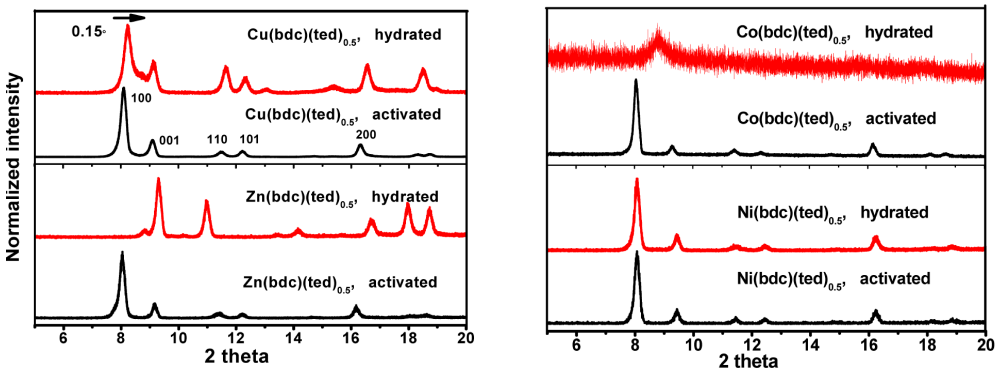

Figure 3. Powder X-ray patterns of activated (pristine) and hydrated M(bdc)(ted)$_{0.5}$ [M = Cu, Zn, Co and Ni] after exposure to 9.5 Torr of D_2O vapor. (Reprinted with permission from Ref. [43]. © 2012 American Chemical Society).

bottom panel of Figure 3 clearly indicates that the Zn(bdc)(ted)$_{0.5}$ system transforms into MOF2 after hydration. This transformation starts with the detachment of the ted group and the subsequent bonding of the D_2O molecules to the Zn^{2+} apical sites of the paddle-wheel building units through their oxygen atoms. Concerning the Ni(bdc)(ted)$_{0.5}$ and Co(bdc)(ted)$_{0.5}$ systems under humid conditions, the right bottom and right upper panels of Figure 3 indicate that the Ni(bdc)(ted)$_{0.5}$ maintains its structure after been exposed to 9.5 Torr of D_2O vapor, while the Co(bdc)(ted)$_{0.5}$ is completely destroyed after exposure. Furthermore, the Co(bdc)(ted)$_{0.5}$ structure cannot be recovered after annealing in vacuum up to 150°C, see Figure S13 in the supplemental material of Ref. [43].

In order to explain the previous experimental results and give a clear explanation of how water interacts with the M(bdc)(ted)$_{0.5}$, we review computational results obtained in Ref. [43] concerning the Ni(bdc)(ted)$_{0.5}$ and Zn(bdc)(ted)$_{0.5}$ systems. The energy ΔE needed to extract the paddle wheel and replace it with water molecules was calculated using the vdW-DF formalism as

$$\begin{aligned}\Delta E_{\mathrm{M(bdc)(ted)_{0.5}}} &= E[\mathrm{M(bdc)(ted)_{0.5}}] + E[n\,\mathrm{H_2O}] \\ &- E[\mathrm{MOF2} + n\,\mathrm{H_2O}] - 1/2\,E[(\mathrm{ted})]\,, \end{aligned} \tag{3}$$

where n is the number of water molecules in the MOF, E[M(bdc)(ted)$_{0.5}$] is the energy of the MOF with no water molecules in it (as seen in the left panel of Figure 2), $E[n\,\mathrm{H_2O}]$ is the energy of n water molecules, $E[\mathrm{MOF2} + n\,\mathrm{H_2O}]$ is the energy of the M(bdc)(ted)$_{0.5}$ where the "exiting" ted has been replaced with n water molecules (right panel of Figure 2) and $E[(\mathrm{ted})]$ is the energy of the ted. Table 2 shows the energies required to substitute the ted in the Zn and Ni(bdc)(ted)$_{0.5}$ structures by 2, 4, 6, 8, and 10 water molecules. Note that negative ΔE values indicate that the replacement is energetically favorable. The table shows that Ni(bdc)(ted)$_{0.5}$ is more resistant to water than Zn(bdc)(ted)$_{0.5}$, as found in the spectra in Figure 3, and the hydration of the latter is a spontaneous process. This is due to the strong H bonds between the water molecules, which stabilizes the coordination of the Zn metal centers. On the other hand,

Table 2. Computed $\Delta E_{\mathrm{M(bdc)(ted)_{0.5}}}$ and $\Delta E_{\mathrm{M\text{-}MOF2}}$ (kJ mol^{-1} cell^{-1}) as a function of the number of water molecules per cell. Note that the basic MOF2 structure already contains two water molecules. Data taken from Ref. [43].

	$\Delta E_{\mathrm{M(bdc)(ted)_{0.5}}}$			$\Delta E_{\mathrm{M\text{-}MOF2}}$		
H_2O/cell	Zn	Ni	Δ	Zn	Ni	Δ
2	43.1	85.5	42.4	—	—	—
4	–5.3	4.2	9.5	–53.6	–77.1	–23.5
6	–21.4	–17.1	4.3	–53.7	–68.4	–14.7
8	–31.3	–24.0	7.3	–56.1	–52.4	3.7
10	–35.0	–45.2	–10.2	–54.5	–55.3	–0.8

in the case of Ni(bdc)(ted)$_{0.5}$, $\Delta E_{\mathrm{M(bdc)(ted)_{0.5}}}$ becomes negative only when the number of water molecules is 6 or greater.

Alternatively, one can calculate the energy $\Delta E_{\mathrm{M\text{-}MOF2}}$ required for hydration of the MOF2 structure with n water molecules, using:

$$\begin{aligned}\Delta E_{\mathrm{M\text{-}MOF2}} = {} & E[\mathrm{MOF2}] + E[n\,\mathrm{H_2O}] \\ & - E[\mathrm{MOF2} + n\,\mathrm{H_2O}]\ . \end{aligned} \tag{4}$$

Here, E[MOF2] is the energy of the M(bdc)(ted)$_{0.5}$, where the ted has been replaced by two molecules of water; the other terms in the equation have been previously defined, see Equation 3. The right hand side of Table 2 shows that for MOF2 the hydration of the Zn and Ni systems is a spontaneous process with an energy gain of approximately -55 kJ mol^{-1} cell^{-1} for higher loadings. This trend is almost independent of the metal.

In conclusion, the computational results explain the experimental findings in Ref. [43], indicating that the structural stability of the system depends on the amount of water present in the MOF. At lower loadings the system is stable, while at higher loadings the interaction of water with the paddle wheel leads to the irreversible decomposition of the structure.

4.3. Studying the formation of water clusters in fluorinated MOFs

The large internal surface area of MOFs makes them ideal for catalysis and fuel cell applications, which have attracted a surge of interest [10–12, 16, 114, 115]. While some progress has been made—for example, Hurd et al. [116] show intriguing results for β-PCMOF2 (proton conducting metal organic framework 2), capable of proton transport under anhydrous conditions at 150°C—in general, the low hydrothermal and chemical stability of MOFs prevents their implementation in catalytic and fuel-cells systems. In the recent past, thus, concerted efforts have focused on increasing the hydrothermal and chemical stability of MOFs [109, 117, 118].

A promising approach to increase the chemical and hydrothermal stability is fluorinated MOFs (FMOFs), where the H atoms have been replaced by F atoms

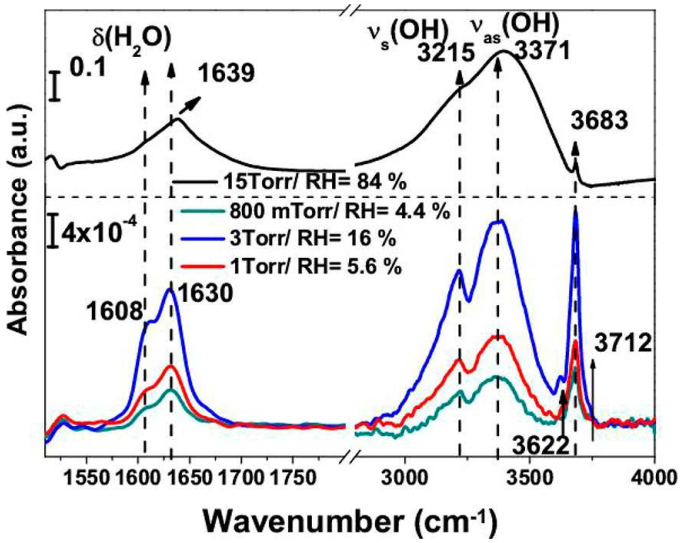

Figure 4. IR absorption spectra of water exposure in FMOF1 as a function of pressure. Absorption spectra are referenced to dehydrated FMOF1 in vacuum. The top panel shows exposure at 15 Torr, while the bottom part shows exposure at lower pressures (800 mTorr to 3 Torr). (Reprinted with permission from Ref. [24]. © 2013 American Chemical Society).

[119–121]. Yang et al. report interesting results for FMOF1, showing that the hydrogen-desorption isotherm does not follow the path of the adsorption isotherm [119], in fact, it shows an abrupt drop in the adsorption density at 14 bar. The authors highlight the fact that this behavior would allow FMOF1 to adsorb H_2 at high pressures and stored it at low pressures.

In general, the walls of FMOF systems are hydrophobic, leading to an interesting side effect: the weak interaction of water molecules with the FMOF enhances the creation of water clusters inside its pores. In this subsection, we review the formation and behavior of water clusters inside FMOF1, as reported in Ref. [24]. As in previous sections, an understanding of the weak molecular interactions inside this system was gained by a combination of vdW-DF calculations and IR absorption spectra of water exposed FMOF1 as a function of pressure. Note that the interaction between water molecules has a significant van der Waals component, which is well captured with vdW-DF [122], while the electrostatic interaction is suppressed by the wall hydrophobicity of FMOF1.

Experimental isotherm measurements of FMOF1 show that the adsorption of water is negligible compared to the water adsorption in other systems [121]. Furthermore, at low water pressures (800 mTorr to 3 Torr), the IR adsorption measurements of H_2O adsorbed on FMOF1 show two peaks corresponding to red (-13 cm^{-1}) and blue-shifts ($+9$ cm^{-1}) of the unperturbed scissor vibration mode (1621 cm^{-1}) of the water molecule, as can be seen Figure 4. On the other hand, as the pressure is increased to 9 Torr, new peaks associated with scissor vibration modes appear at 1639 cm^{-1} and 1676 cm^{-1}, as can be seen in the top panel of Figure 5.

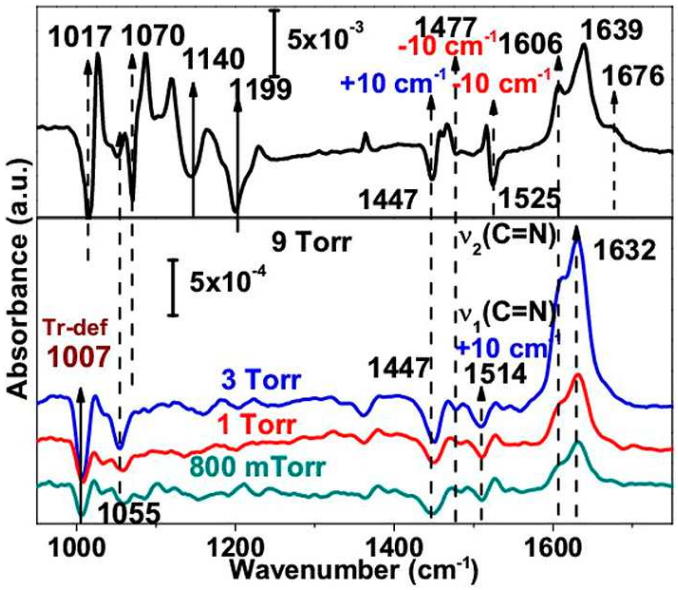

Figure 5. IR absorption spectra of H_2O adsorbed in FMOF1 showing the bending modes of adsorbed water as a function of pressure. Top part shows IR absorption spectrum at 9 Torr. (Reprinted with permission from Ref. [24]. © 2013 American Chemical Society).

In order to elucidate the appearance and nature of these peaks, vdW-DF vibration calculations were performed for various water clusters, i.e. the water dimer, trimer, tetramer, pentamer, and ice; the results are shown in Figure 6. Figure 6a) shows the calculated modes convoluted by Gaussian functions of 20 cm^{-1} bandwidth, while panel b) shows single frequency values represented by peaks of 1 cm^{-1} width. As expected, from the figure it can be seen that the bigger the water cluster, the higher the number of scissors modes. It is also important to note that for pressures under 3 Torr, the scissor vibrational modes in Figure 4 span from 1600 cm^{-1} to 1650 cm^{-1}. This matches the theoretical frequency windows of both the tetramer and pentamer, as seen in the top panel of Figure 6. It follows that the water clusters formed inside FMOF1 under low pressures ($<$ 3 Torr) are comprised of no more than 5 water molecules. This conclusion is also supported by the water adsorption energies on the FMOF1, see Table 2 in Ref. [24]. Note that, in principle, up to 61 water molecules can be accommodated inside the pores of FMOF1. On the other hand, the experimentally observed peak located at 1676 cm^{-1} in Figure 5 can be associate with hydrogen-bonded water molecules or water clusters larger than five water molecules—see the orange line in the top panel of Figure 6. It is important to note that this peak is only visible at high pressures.

In summary, while the IR spectroscopy data of water-exposed FMOF1 showed the appearance of new peaks, it was only with the help of vdW-DF calculations that a clear assignment to particular water clusters could be made. Note that this finding is likely to have a tremendous impact on atmospheric sciences, which seek to study the existence and properties of such clusters. In the normal atmosphere, water cluster

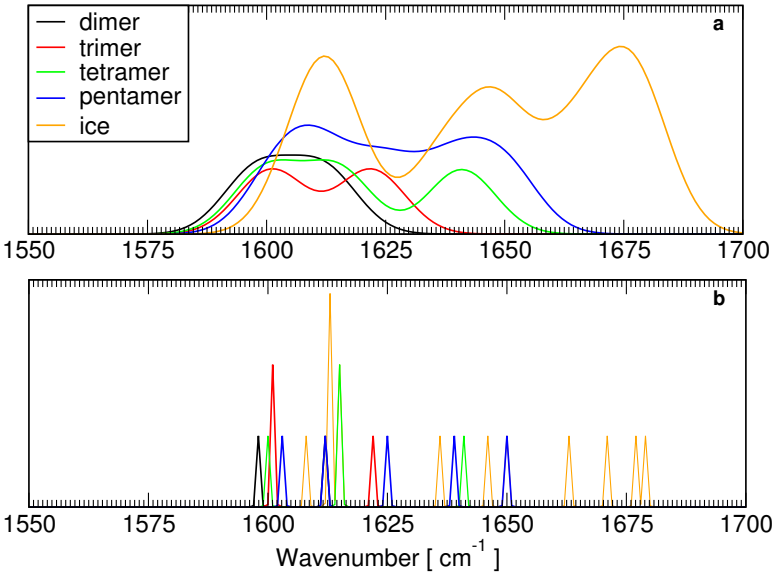

Figure 6. a) Gaussian convolution (with bandwidth of 20 cm^{-1}) of bending mode frequencies for various cluster sizes. b) Single frequency values represented by peaks of 1 cm^{-1} width, as reported by previous vdW-DF calculations on gas-phase water clusters [122]. (Reprinted with permission from Ref. [24]. © 2013 American Chemical Society).

concentration decays exponentially with the aggregate size, making clusters larger than the trimer often difficult to observe. FMOF1 solves this problem and provides a simple environment to create and confine even larger clusters.

4.4. Studying small molecule diffusion in MOFs

MOFs have attracted a lot of attention due their promising properties concerning the storage of hydrogen and capture of CO_2 [9], among others. However, for the effectiveness of all such applications, it is necessary to get guest molecules deep into the bulk of the MOF, or vice versa, have them diffuse out. As such, the diffusivity of the guest molecule through the porous material plays a major role in these processes and is critical for the understanding and rational design of new MOFs. The topic of small molecule diffusion in MOFs has thus been the target of many theoretical studies [123–129]. For example, in Ref. [128] Haldoupis et al. identified key elements in the MOF's pore structure and via molecular dynamic simulations they were able to predict the Henry constant and the activation energy for several guest molecules. In particular, the authors were able to identify several materials with promising properties towards the separation of gases, such as H_2, CO_2, and CH_4. However, in their study, the authors assume that the MOFs are rigid structures, which can be a serious limitation, as we know that some MOFs experience a significant change in their structure upon adsorption of the guess molecules or other external stimuli due to their high flexibility.

In this subsection we review a combined *in situ* IR/vdW-DF study of small molecule diffusion in Mg-MOF74, as described in [87]. MOF74 was chosen for this study due to

Table 3. Adsorption energies ΔE of molecules in Mg-MOF74 in eV. Two different loading are considered, i.e. one molecule per unit cell (low loading) and 6 molecules per unit cell (high loading). In addition, adsorption energies corrected for the zero-point energy (ΔE_{ZPE}) and thermal contribution (ΔH_{298} at 298 K) are given in eV. Data taken from Ref. [87].

Molecule	Loading	ΔE	ΔE_{ZPE}	H_{298}
H_2	1	–0.15	–0.15	–0.15
	6	–0.16	–0.16	–0.16
CO_2	1	–0.50	–0.49	–0.50
	6	–0.50	–0.49	–0.50
H_2O	1	–0.79	–0.76	–0.76
	6	–0.76	–0.73	–0.73

its unsaturated metal centers, which makes it highly reactive towards the adsorption of small molecules. Furthermore, Mg-MOF74 has shown promising properties towards the adsorption of CO_2 compared to other MOFs.

We start by showing results concerning the adsorption energies of H_2, CO_2, and H_2O in the Mg-MOF74 structure, see Table 3. This table shows that for low to moderate loadings the interaction between adsorbate molecules is negligible, except for H_2O adsorption, where the repulsion between the H atoms of the water molecules slightly debilitates the H_2O binding to the MOF. The adsorption energies for the adsorption of H_2 and CO_2, obtained using the vdW-DF approach, are in excellent agreement with the experimental values of -0.11 ± 0.003 eV [98] and -0.49 ± 0.010 eV [104], respectively. Although not the focus of that particular study, Table 3 also reveals a common problem of many MOFs: the adsorption energy of water (due to its large dipole moment) is typically significantly higher compared to e.g. H_2 and CO_2. Thus, the presence of even small traces of water is a serious impediment upon possible applications and devices, as anticipated in the previous section. Details about this problem are discussed in Ref. [90]. In addition to adsorption energies, calculations of the vibrational spectra show a frequency change after adsorption of $\Delta\nu_{\mathrm{H_2}} = -30$ cm^{-1}, $\Delta\nu_{\mathrm{CO_2}} = -13$ cm^{-1}, and $\Delta\nu_{\mathrm{H_2O}} = -103$ cm^{-1}, in remarkable agreement with the IR spectroscopy measurement of $\Delta\nu_{\mathrm{H_2}} = -36$ cm^{-1}, $\Delta\nu_{\mathrm{CO_2}} = -8$ cm^{-1}, and $\Delta\nu_{\mathrm{H_2O}} = -99$ cm^{-1}. Experimentally, there is also a small difference in frequency change between low and high loading, resulting in a red-shift of -3 cm^{-1} and -15 cm^{-1} for the asymmetric stretch modes of CO_2 and H_2O (see Supplemental Material of Ref. [87]). Computationally, we find $\Delta\nu_{\mathrm{CO_2}} = -1$ cm^{-1} and $\Delta\nu_{\mathrm{H_2O}} = -18$ cm^{-1}, again in excellent agreement with experiment.

The diffusion of small molecules (H_2, CO_2, and H_2O) through the MOF is a complex process. An appropriate description of such processes typically requires computationally expensive first-principle molecular dynamic simulations. However, here we were able to avoid the use of molecular dynamics by finding four different diffusion paths that capture important molecular transport mechanisms responsible for the macroscopic diffusion of H_2, CO_2, and H_2O in the MOF structure. These four paths are: a) The guest molecule,

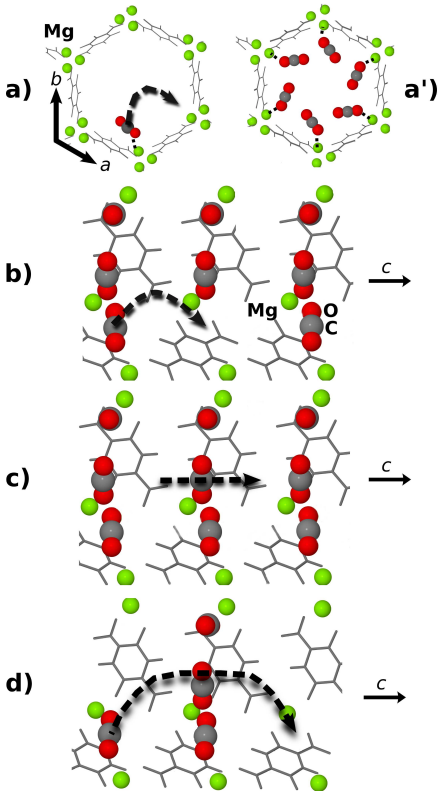

Figure 7. Graphical representation of the diffusion mechanisms considered in this study, shown for the case of CO_2. a) and a') are views directly along the *c*-axis of the hexagonal Mg-MOF74 cell, where one (low loading) and six CO_2 (high loading) are adsorbed. b), c), and d) are views perpendicular to the *c*-axis. In panel b) the guest molecule, adsorbed on a metal center, diffuses along the *c*-axis to the next metal center. In panel c) the guest molecule travels along the center of the MOF channel, while all the metal centers are occupied by the same type of guest molecule. In panel d) the guest molecule, adsorbed on one of the metal centers, travels along the *c*-axis through a barrier made of other adsorbed molecules and is adsorbed again at the equivalent metal center two unit cells further down. Dashed lines indicate the diffusion paths. (Reprinted with permission from Ref. [87]. © 2012 American Physical Society).

adsorbed on one metal center, travels circularly from one metal center to the next. Note that this mechanism is not responsible for molecular transport into the MOF, but nevertheless is an important process for redistributing the molecular load. b) The guest molecule, adsorbed on the metal center, diffuses along the *c*-axis to the next metal center. c) The guest molecule travels through the center of the MOFs channel, where all the metal centers are occupied by the same type of guest molecules. And, d) the guest molecule, adsorbed on one of the metal centers, travels along the *c*-axis through a barrier made by adsorbed molecules and is adsorbed at the equivalent metal center two unit cell further down. See Figure 7 for a graphical representation of these four diffusion paths. For these paths, diffusion barriers were then calculated utilizing vdW-DF combined with the climbing-image nudged elastic band (NEB) approach.

The energy barriers of the four diffusion paths are plotted in Figure 8. Note that

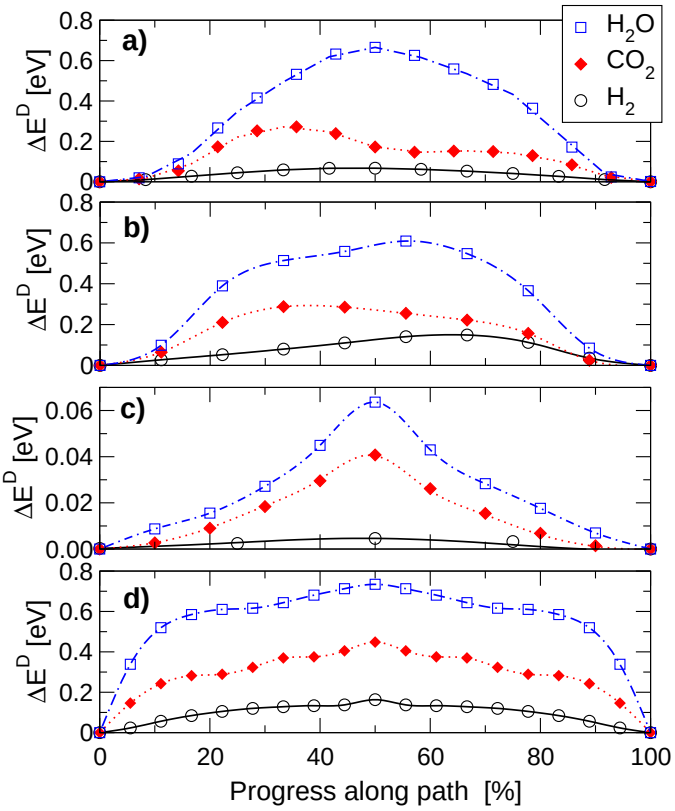

Figure 8. Diffusion profiles (in eV) for the diffusion processes of H_2, CO_2, and H_2O in Mg-MOF74 according to the mechanisms in Figure 7. (Reprinted with permission from Ref. [87]. © 2012 American Physical Society).

diffusion barriers corrected for the zero-point energy were also calculated, but are not reproduced here. From the figure it can be seen that water has the highest energy barrier for diffusion. Again, the presence of water inside the MOF is a serious issue, as the barrier for it to diffuse out is rather large. As expected, the energy barriers are comparable to the adsorption energies. In panel a), it can be seen that a local minimum is located at 58% of the path for CO_2 diffusion. This local minimum has its origins in the presence of a secondary adsorption site in the MOF. Due to its low depth (5 meV), the secondary adsorption site is only occupied at high loadings. This secondary adsorption site for the CO_2 molecule was first reported by Queen et al. in Ref. [130], where the authors conducted neutron powder diffraction experiments on the Mg-MOF74 as a function of the CO_2 loading. Paths b), c), and d) aim to simulate the diffusion of the guest molecule into the MOF. Note that the diffusion barrier in path c) are ten times lower than the ones obtained in paths a), b) and d). This indicates that the interaction between the guest molecules in the middle of the channel and the ones adsorbed at the metals sites is small. Furthermore, it is important to highlight that the diffusion energy barrier of CO_2 in Figure 8c), i.e. 0.04 eV, becomes 0.03 eV when corrected for the zero-point energy. This value is in excellent agreement with the 0.03 eV energy barrier measured experimentally by Bao et al. in Ref. [131].

In addition to vdW-DF calculations, *in situ* IR time-resolved spectroscopy measurements of the diffusion of CO_2 and H_2O in Mg-MOF74 were performed. When the experiments were first performed, the results were difficult to understand. In the case of CO_2, at first we observed a red-shift in the vibration frequency (asymmetric mode) of the guest molecule. As time passes, the IR spectrum measurements show a second shift (blue-shift) in the vibration frequencies of the guest molecules, leading to the original IR spectrum. The analogous behavior is observed for the corresponding experiment with H_2O. With the help of theory, we were able to construct a model that explains these effects. At first, molecules entering the MOF mostly adsorb in the pores close to the surface and "clog" those. This causes the first experimentally observed red-shift. Those pores become highly loaded, which we were able to deduce from the calculated difference in frequency shift from the low- and high-loading situations. Then, after some time, molecules start to diffuse deeper into the MOF using mechanism c), diffusing from pores with high concentration of guest molecules to pores with lower concentration. This results in the second shift observed, i.e. blue shifting back to the original spectrum.

To test our model, we compare the experimental timescale for the CO_2 and H_2O cases. The experiments show that it takes approximately two hours for the H_2O molecules and 22 minutes for the CO_2 molecules to go from the high-loading regime to the low-loading regime. The ratio between these two times is 5.45. On the other hand, having calculated the corresponding diffusion barriers (and calculating the pre-exponential factor in the Arrhenius equation with the help of transition-state theory), we can compute the same ratio and find purely based on our *ab initio* calculations a value of 5.43, validating our theoretical accuracy and transport model.

In summary, as in the previous subsections, only the combination of experiment and theory was able to present a complete picture of small molecule diffusion in MOF74. The theoretical atomistic model for the molecular transport explains experimental IR macroscopic evidence. The simulations also clarify the two-state mechanism, observed experimentally, which controls the macroscopic diffusion of these molecules in MOF74.

5. Summary and Outlook

In this work, we have shown several examples of how the synergy of IR and Raman spectroscopy techniques, together with *ab initio* calculations at the DFT level utilizing vdW-DF, allow us to give a complete description of the van der Waals binding and interaction between guest molecules and the MOF. While originally many studies of MOFs focused on adsorption of H_2 and CO_2, at the moment we see a vast expansion of this field, including many other molecules of interest, such as SO_2 and NO_2 [89,132–135]. Interesting effects are also being studied, such as a pressure dependent gate opening of MOFs [48, 136–138] and the response of MOFs to a variety of external stimuli. Due to the versatile building-block nature of MOFs, an almost innumerable number of MOFs might exist. But, more fundamental research is necessary to understand their properties

and tailor them according to our needs. Nonetheless, and at this point we probably only have seen a glimpse of their applicability for future applications and devices.

Acknowledgment

This work was entirely supported by Department of Energy Grant No. DE-FG02-08ER46491.

References

[1] Dan Zhao, Daqiang Yuan, and Hong-Cai Zhou. The current status of hydrogen storage in metal-organic frameworks. *Energy and Environmental Science*, 1:222–235, 2008.

[2] Daofeng Sun, Shengqian Ma, Yanxiong Ke, David J. Collins, and Hong-Cai Zhou. An interweaving mof with high hydrogen uptake daofeng. *Journal of the American Chemical Society*, 128:3896–3897, 2006.

[3] Nathaniel L Rosi, Juergen Eckert, Mohamed Eddaoudi, David T Vodak, Jaheon Kim, Michael O'Keeffe, and Omar M. Yaghi. Hydrogen storage in microporous metal-organic frameworks. *Science*, 300:1127–11279, 2003.

[4] Hiroyasu Furukawa, Michael A. Miller, and Omar M. Yaghi. Independent verification of the saturation hydrogen uptake in mof-177 and establishment of a benchmark for hydrogen adsorption in metal-organic frameworks. *Journal of Materials Chemistry*, 17:3197–3204, 2007.

[5] Jihyun An and Nathaniel L Rosi. Tuning mof co2 adsorption properties via cation exchange. *Journal of the American Chemical Society*, 132:5578–5579, 2010.

[6] Jian Liu, Praveen K. Thallapally, B. Peter McGrail, Daryl R. Brown, and Jun Liu. Progress in adsorption-based co_2 capture by metal-organic frameworks. *Chemical Society reviews*, 41:2308–2322, 2012.

[7] Arijit Mallick, Subhadeep Saha, Pradip Pachfule, Sudip Roy, and Rahul Banerjee. Selective co_2 and h_2 adsorption in a chiral magnesium-based metal organic framework (mg-mof) with open metal sites. *Journal of Materials Chemistry*, 20:9073–9080, 2010.

[8] Lukás Grajciar, Andrew D Wiersum, Philip L. Llewellyn, Jong-san Chang, and Petr Nachtigall. Understanding co_2 adsorption in cubtc mof : Comparing combined dft-ab initio calculations with microcalorimetry experiments. *The Journal of Physical Chemistry C*, 115:17925–17933, 2011.

[9] Marc Pera-Titus. Porous inorganic membranes for co_2 capture: Present and prospects. *Chemical Reviews*, 114:1413–1492, 2014.

[10] Omar K. Farha, Abraham M. Shultz, Amy A. Sarjeant, SonBinh T. Nguyen, and Joseph T. Hupp. Active-site-accessible, porphyrinic metal-organic framework materials. *Journal of the American Chemical Society*, 133:5652–5655, 2011.

[11] JeongYong Lee, Omar K. Farha, John Roberts, Karl A. Scheidt, SonBinh T. Nguyen, and Joseph T. Hupp. Metal-organic framework materials as catalysts. *Chemical Society reviews*, 38:1450–1459, 2009.

[12] Abraham M. Shultz, Omar K. Farha, Joseph T. Hupp, and SonBinh T. Nguyen. A catalytically active, permanently microporous mof with metalloporphyrin struts. *Journal of the American Chemical Society*, 131:4204–4205, 2009.

[13] Lauren E. Kreno, Kirsty Leong, Omar K. Farha, Mark Allendorf, Richard P. Van Duyne, and Joseph T. Hupp. Metal-organic framework materials as chemical sensors. *Chemical Reviews*, 112:1105–1125, 2012.

[14] A. Stroppa, P. Barone, P. Jain, J. M. Perez-Mato, and S. Picozzi. Hybrid improper ferroelectricity in a multiferroic and magnetoelectric metal organic framework. *Advanced Materials*, 25(16):2284–2290, 2013.

[15] Alessandro Stroppa, Prashant Jain, Paolo Barone, Martijn Marsman, Juan Manuel Perez-Mato, Anthony K. Cheetham, Harold W. Kroto, and Silvia Picozzi. Electric control of magnetization and interplay between orbital ordering and ferroelectricity in a multiferroic metal organic framework. *Angewandte Chemie International Edition*, 50:5847–5850, 2011.

[16] Ryan J. Kuppler, Daren J. Timmons, Qian-Rong Fang, Jian-Rong Li, Trevor A. Makal, Mark D. Young, Daqiang Yuan, Dan Zhao, Wenjuan Zhuang, and Hong-Cai Zhou. Potential applications of metal-organic frameworks. *Coordination Chemistry Reviews*, 253:3042–3066, 2009.

[17] Norbert Stock and Shyam Biswas. Synthesis of metal-organic frameworks (mofs): Routes to various mof topologies, morphologies, and composites. *Chemical Reviews*, 112:933–969, 2012.

[18] Jesse L. C. Rowsell, A. R. Millward, K. S. Park, and O. M. Yaghi. Hydrogen sorption in functionalized metal-organic frameworks. *Journal of the American Chemical Society*, 126:5666–5667, 2004.

[19] Qingyuan Yang, Sébastien Vaesen, Florence Ragon, Andrew D. Wiersum, Dong Wu, Ana Lago, Thomas Devic, Charlotte Martineau, Francis Taulelle, Philip L Llewellyn, Hervé Jobic, Chongli Zhong, Christian Serre, Guy De Weireld, and Guillaume Maurin. A water stable metal-organic framework with optimal features for co2 capture. *Angewandte Chemie International Eddition*, 52:10316–10320, 2013.

[20] Jared M. Taylor, Karl W. Dawson, and George K. H. Shimizu. A water-stable metal-organic framework with highly acidic pores for proton-conducting applications. *Journal of the American Chemical Society*, 135:1193–1196, 2013.

[21] Yameng Li, Zhanfeng Ju, Benlai Wu, and Daqiang Yuan. A water and thermally stable metal-organic framework featuring selective co_2 adsorption. *Crystal Growth & Design*, 13(9):4125–4130, 2013.

[22] Sang Soo Han, Seung-Hoon Choi, and Adri C. T. van Duin. Molecular dynamics simulations of stability of metal-organic frameworks against h_2o using the reaxff reactive force field. *Chemical communications*, 46:5713–5715, 2010.

[23] Aude Demessence, Deanna M. DAlessandro, Maw Lin Foo, and Jeffrey R. Long. Strong co2 binding in a water-stable, triazolate-bridged metalorganic framework functionalized with ethylenediamine. *Journal of the American Chemical Society*, 131(25):8784–8786, 2009. PMID: 19505094.

[24] Nour Nijem, Pieremanuele Canepa, Ushasree Kaipa, Kui Tan, Katy Roodenko, Sammer Tekarli, Jason Halbert, Iain W. H. Oswald, Ravi K. Arvapally, Chi Yang, Timo Thonhauser, Mohammad a Omary, and Yves J Chabal. Water cluster confinement and methane adsorption in the hydrophobic cavities of a fluorinated metal-organic framework. *Journal of the American Chemical Society*, 135:12615–12626, 2013.

[25] M. Dion, H. Rydberg, E. Schröder, D. C. Langreth, and B. I. Lundqvist. Van der waals density functional for general geometries. *Physical Review Letters*, 92:246401, 2004.

[26] T. Thonhauser, Valentino R. Cooper, Shen Li, Aaron Puzder, Per Hyldgaard, and David C. Langreth. Van der waals density functional: Self-consistent potential and the nature of the van der waals bond. *Physical Review B*, 76:125112, 2007.

[27] Kyuho Lee, amonn D. Murray, Lingzhu Kong, Bengt I. Lundqvist, and David C. Langreth. Higher-accuracy van der waals density functional. *Physical Review B*, 82:081101, 2010.

[28] K Nakamot. *Infrared and Raman Spectra of Inorganic and Coordination Compounds*. 6th ed. Wiley & Sons, Hoboken, New Jersey, United States, 2009.

[29] JR Ferraro, K Nakamoto, and CW Brown. *Introductory Raman Spectroscopy*. 2nd ed Academic Press, San Diego, California, 2003.

[30] H. L. Welsh. The pressure-induced infrared spectrum of hydrogen and its application to the study of planetary atmospheres. *Journal of the Atmospheric Sciences*, 26:835–840, 1969.

[31] Carlo Lamberti, Adriano Zecchina, Elena Groppo, and Silvia Bordiga. Probing the surfaces of heterogeneous catalysts by in situ ir spectroscopy. *Chemical Society Reviews*, 39:4951–5001, 2010.

[32] Alexandre Vimont, Arnaud Travert, Philippe Bazin, Jean-Claude Lavalley, Marco Daturi, Christian Serre, Gerard Ferey, Sandrine Bourrelly, and Philip L. Llewellyn. Evidence of co_2 molecule acting as an electron acceptor on a nanoporous metal-organic-framework mil-53 or cr_3+(oh)(o_2c-c_6h_4-co_2). *Chemical Communications*, pages 3291–3293, 2007.

[33] Jorge Gascon, Ugur Aktay, Maria D. Hernandez-Alonso, Gerard P.M. van Klink, and Freek Kapteijn. Amino-based metal-organic frameworks as stable, highly active basic catalysts. *Journal of Catalysis*, 261:75–87, 2009.

[34] Eli Stavitski, Evgeny A. Pidko, Sarah Couck, Tom Remy, Emiel J. M. Hensen, Bert M. Weckhuysen, Joeri Denayer, Jorge Gascon, and Freek Kapteijn. Complexity behind co2 capture on nh2-mil-53(al). *Langmuir*, 27(7):3970–3976, 2011.

[35] J.Cz. Dobrowolski and M.H. Jamroz. Infrared evidence for co_2 electron donor-acceptor complexes. *Journal of Molecular Structure*, 275:211–219, 1992.

[36] Sergei G. Kazarian, Michael F. Vincent, Frank V. Bright, Charles L. Liotta, and Charles A. Eckert. Specific intermolecular interaction of carbon dioxide with polymers. *Journal of the American Chemical Society*, 118(7):1729–1736, 1996.

[37] Nour Nijem, Jean-François Veyan, Lingzhu Kong, Kunhao Li, Sanhita Pramanik, Yonggang Zhao, Jing Li, David Langreth, and Yves J. Chabal. Interaction of molecular hydrogen with microporous metal organic framework materials at room temperature. *Journal of the American Chemical Society*, 132(5):1654–1664, 2010.

[38] Nour Nijem, Jean-François Veyan, Lingzhu Kong, Haohan Wu, Yonggang Zhao, Jing Li, David C. Langreth, and Yves J. Chabal. Molecular hydrogen "pairing" interaction in a metal organic framework system with unsaturated metal centers (mof-74). *Journal of the American Chemical Society*, 132(42):14834–14848, 2010.

[39] S. Bordiga, L. Regli, F. Bonino, E. Groppo, C. Lamberti, B. Xiao, P. S. Wheatley, R. E. Morris, and A. Zecchina. Adsorption properties of hkust-1 toward hydrogen and other small molecules monitored by ir. *Physical Chemistry Chemical Physics*, 9:2676–2685, 2007.

[40] Jenny G. Vitillo, Laura Regli, Sachin Chavan, Gabriele Ricchiardi, Giuseppe Spoto, Pascal D. C. Dietzel, Silvia Bordiga, and Adriano Zecchina. Role of exposed metal sites in hydrogen storage in mofs. *Journal of the American Chemical Society*, 130(26):8386–8396, 2008. PMID: 18533719.

[41] Edoardo Garrone and Carlos Otero Arean. Variable temperature infrared spectroscopy: A convenient tool for studying the thermodynamics of weak solid-gas interactions. *Chemical Society Reviews*, 34:846–857, 2005.

[42] Silvia Bordiga, Jenny G. Vitillo, Gabriele Ricchiardi, Laura Regli, Donato Cocina, Adriano Zecchina, Bjørnar Arstad, Morten Bjørgen, Jasmina Hafizovic, and Karl Petter Lillerud. Interaction of hydrogen with mof-5. *The Journal of Physical Chemistry B*, 109(39):18237–18242, 2005.

[43] Kui Tan, Nour Nijem, Pieremanuele Canepa, Qihan Gong, Jing Li, Timo Thonhauser, and Yves J. Chabal. Stability and hydrolyzation of metal organic frameworks with paddle-wheel sbus upon hydration. *Chemistry of Materials*, 24:3153–3167, 2012.

[44] Stephen A. FitzGerald, Brian Burkholder, Michael Friedman, Jesse B. Hopkins, Christopher J. Pierce, Jennifer M. Schloss, Benjamin Thompson, and Jesse L. C. Rowsell. Metal-specific interactions of h_2 adsorbed within isostructural metal-organic frameworks. *Journal of the American Chemical Society*, 133(50):20310–20318, 2011.

[45] S. A. FitzGerald, J. Hopkins, B. Burkholder, M. Friedman, and J. L. C. Rowsell. Quantum dynamics of adsorbed normal- and para-h_2, hd, and d_2 in the microporous framework mof-74 analyzed using infrared spectroscopy. *Phys. Rev. B*, 81:104305, Mar 2010.

[46] Charles F. Jr. Windisch, Praveen K. Thallapally, and B. Peter McGrail. Adsorption of co_2 on $co_3^{II}[co^{III}(cn)_6]_2$ using drifts. *Spectrochimica Acta Part A: Molecular and Biomolecular Spectroscopy*, 74(3):629–634, 2009.

[47] Nour Nijem, Peter Thissen, Yanpeng Yao, Roberto C. Longo, Katy Roodenko, Haohan

Wu, Yonggang Zhao, Kyeongjae Cho, Jing Li, David C. Langreth, and Yves J Chabal. Understanding the preferential adsorption of co_2 over n_2 in a flexible metal-organic framework. *Journal of the American Chemical Society*, 133:12849–12857, 2011.

[48] Nour Nijem, Haohan Wu, Pieremanuele Canepa, Anne Marti, Kenneth J. Balkus, Timo Thonhauser, Jing Li, and Yves J. Chabal. Tuning the gate opening pressure of metal-organic frameworks (mofs) for the selective separation of hydrocarbons. *Journal of the American Chemical Society*, 134:15201–15204, 2012.

[49] Brian Kolb and T. Thonhauser. Molecular Biology At the Quantum Level: Can Modern Density Functional Theory Forge the Path? *Nano LIFE*, 02(02):1230006, June 2012.

[50] A. Szabo and N. S. Ostlund. *Modern Quantum Chemistry: Introduction to Advanced Electronic Structure Theory*. Dover, Mineola, New York, 1996.

[51] M. Head-Gordon and E. Artacho. Chemistry on the computer. *Physics Today*, 61:58–63, 2008.

[52] M. Marsman, A. Grüneis, J. Paier, and G. Kresse. Second-order møller-plesset perturbation theory applied to extended systems. i. within the projector-augmented-wave formalism using a plane wave basis set. *The Journal of Chemical Physics*, 130(18):184103, 2009.

[53] George H. Booth, Andreas Gruneis, Georg Kresse, and Ali Alavi. Towards an exact description of electronic wavefunctions in real solids. *Nature*, 493:365–370, 2012.

[54] Andreas Grüneis, Martijn Marsman, and Georg Kresse. Second-order møller-plesset perturbation theory applied to extended systems. ii. structural and energetic properties. *The Journal of Chemical Physics*, 133(7):074107, 2010.

[55] Denis Usvyat, Bartolomeo Civalleri, Lorenzo Maschio, Roberto Dovesi, Cesare Pisani, and Martin Schütz. Approaching the theoretical limit in periodic local mp2 calculations with atomic-orbital basis sets: The case of lih. *The Journal of Chemical Physics*, 134(21):2141050, 2011.

[56] Philippe Y. Ayala, Konstantin N. Kudin, and Gustavo E. Scuseria. Atomic orbital laplace-transformed second-order møller-plesset theory for periodic systems. *The Journal of Chemical Physics*, 115(21):9698–9707, 2001.

[57] Lorenzo Maschio, Denis Usvyat, Frederick R. Manby, Silvia Casassa, Cesare Pisani, and Martin Schütz. Fast local-mp2 method with density-fitting for crystals. i. theory and algorithms. *Phys. Rev. B*, 76:075101, Aug 2007.

[58] P. Hohenberg and W. Kohn. Inhomogeneous electron gas. *Physical Review*, 136:B864–B87, 1964.

[59] S. A. Shevlin and Z. X. Guo. Density functional theory simulations of complex hydride and carbon-based storage materials. *Chemical Society Reviews*, 38:211–225, 2009.

[60] P. Hobza. Stacking interaction. *Physical Chemistry Chemical Physics*, 10:2581–2583, 2008.

[61] J. Šponer, K. E. Riley, and P. Hobza. Nature and magnitude of aromatic stacking of nucleic acid bases. *Physical Chemistry Chemical Physics*, 10:2595–2610, 2008.

[62] J. Černý and P. Hobza. Non-covalent interactions in biomacromolecules. *Physical Chemistry Chemical Physics*, 9:5291–5303, 2007.

[63] D. C. Langreth, B. I. Lundqvist, V. R. Chakarova-Käck, S. D.and Cooper, M. Dion, P. Hyldgaard, A. Kelkkanen, L. Kleis, J.and Kong, S. Li, P. G. Moses, E. Murray, A. Puzder, H. Rydberg, E. Schröder, and T. Thonhauser. A density functional for sparse matter. *Journal of Physics: Condensed matter*, 21:084203, 2009.

[64] R. H. French, V. A. Parsegian, R. Podgornik, R. F. Rajter, A. Jagota, J. Luo, D. Asthagiri, M. K. Chaudhury, Y.-M. Chiang, S. Granick, S. Kalinin, M. Kardar, R. Kjellander, D. C. Langreth, J. Lewis, S. Lustig, D. Wesolowski, J. Wettlaufer, W.-Y. Ching, M. Finnis, F. Houlihan, O. A. von Lilienfeld, C. J. van Oss, and T. Zemby. Long range interactions in nanoscale science. *Review of Modern Physics*, 82:1887–1944, 2010.

[65] S. Kristyán and P. Pulay. Can (semi)local density functional theory account for the london dispersion forces? *Chemical Physics Letters*, 229:175–180, 1994.

[66] J. M. Pérez-Jordá, A. D. Becke, and Emilio. San-Fabián. Automatic numerical integration techniques for polyatomic molecules. *Journal of Chemical Physics*, 100:6520–6534, 1994.

[67] E. J. Meijer and M. Sprik. A density-functional study of the intermolecular interactions of

benzene. *Journal of Chemical Physics*, 105:8684–8689, 1996.

[68] S. Grimme. Accurate description of van der waals complexes by density functional theory including empirical corrections. *Journal of Computational Chemistry*, 25:1463–1473, 2004.

[69] S. Grimme. Semiempirical gga-type density functional constructed with a long-range dispersion correction. *Journal of Computational Chemistry*, 27:1787–1799, 2006.

[70] A. Heßelmann and G. Jansen. The helium dimer potential from a combined density functional theory and symmetry-adapted perturbation theory approach using an exact exchange-correlation potential. *Physical Chemistry Chemical Physics*, 5:5010–5014, 2003.

[71] A. J. Misquitta and K. Szalewicz. Intermolecular forces from asymptotically corrected density functional description of monomers. *Chemical Physics Letters*, 357:301–306, 2002.

[72] H. L. Williams and C. F. Chabalowski. Using kohn-sham orbitals in symmetry-adapted perturbation theory to investigate intermolecular interactions. *The Journal of Physical Chemistry A*, 105:646–659, 2001.

[73] A. Tkatchenko and M. Scheffler. Accurate molecular van der waals interactions from ground-state electron density and free-atom reference data. *Physical Review Letters*, 102:073005, 2009.

[74] A. Tkatchenko, R. A. DiStasio Jr., M. Head-Gordon, and M. Scheffler. Dispersion-corrected møller-plesset second-order perturbation theory. *Journal of Chemical Physics*, 131:094106, 2009.

[75] V. R. Cooper, T. Thonhauser, A. Puzder, E. Schröder, B. I. Lundqvist, and D. C. Langreth. Stacking interactions and the twist of dna. *Journal of the American Chemical Society*, 130:1304–1308, 2008.

[76] V. R. Cooper, T. Thonhauser, and D. C. Langreth. An application of the van der waals density functional: Hydrogen bonding and stacking interactions between nucleobases. *Journal of Chemical Physics*, 128:204102, 2008.

[77] H. W. Li, K. Kikuchi, Y. Nakamori, N. Ohba, K. Miwa, S. Towata, and S. Orimo. Dehydriding and rehydriding processes of well-crystallized $mg(bh_4)_2$ accompanying with formation of intermediate compounds. *Acta Materialia*, 56:1342–1347, 2008.

[78] Y. Zhang and W. Yang. Comment on "generalized gradient approximation made simple,". *Physical Review Letters*, 80:890–890, 1998.

[79] J. P. Perdew and Y. Wang. Accurate and simple analytical representation of the electron-gas correlation-energy. *Physical Review B*, 45:13244–13249, 1992.

[80] G. Román-Pérez and J. M. Soler. Efficient implementation of a van der waals density functional: Application to double-wall carbon nanotubes. *Physical Review Letters*, 103:096102, 2009.

[81] A. Bil, B. Kolb, R. Atkinson, D. G. Pettifor, T. Thonhauser, and A. N. Kolmogorov. van der waals interactions in the ground state of $mg(bh_4)_2$ from density functional theory. *Physical Review B*, 83:224103, 2011.

[82] Qi Li, Brian Kolb, Guillermo Román-Pérez, Jose M. Soler, Felix Yndurain, Lingzhu Kong, D. C. Langreth, and T. Thonhauser. Ab initio energetics and kinetics study of h_2 and ch_4 in the si clathrate hydrate. *Physical Review B*, 84:153103, 2011.

[83] Yanpeng Yao, Nour Nijem, Jing Li, Yves J. Chabal, David C. Langreth, and T. Thonhauser. Analyzing the frequency shift of physiadsorbed co_2 in metal organic framework materials. *Physical Review B*, 85:064302, 2012.

[84] Q. Li and T. Thonhauser. A theoretical study of the hydrogen-storage potential of $(h_2)_4ch_4$ in metal organic framework materials and carbon nanotubes. *Journal of physics. Condensed matter*, 24:424204–424211, 2012.

[85] Nour Nijem, Pieremanuele Canepa, Lingzhu Kong, Haohan Wu, Jing Li, Timo Thonhauser, and Yves J. Chabal. Spectroscopic characterization of van der waals interactions in a metal organic framework with unsaturated metal centers: Mof-74-mg. *Journal of physics. Condensed matter*, 24:424203, 2012.

[86] Pieremanuele Canepa, Yves J. Chabal, and T. Thonhauser. When metal organic frameworks turn into linear magnets. *Physical Review B*, 87:094407, 2013.

[87] Pieremanuele Canepa, Nour Nijem, Yves J. Chabal, and T. Thonhauser. Diffusion of small molecules in metal organic framework materials. *Physical Review Letters*, 110:026102, 2013.

[88] M. G. Lopez, Pieremanuele Canepa, and T. Thonhauser. Nmr study of small molecule adsorption in mof-74-mg. *Journal of chemical physics*, 138:154704, 2013.

[89] Kui Tan, Pieremanuele Canepa, Qihan Gong, Jian Liu, Daniel H Johnson, Allison Dyevoich, Praveen K. Thallapally, Timo Thonhauser, Jing Li, and Yves J. Chabal. Mechanism of preferential adsorption of so$_2$ into two microporous paddle wheel frameworks m(bdc)(ted)$_{0.5}$. *Chemistry of Materials*, 25(23):4653–4662, 2013.

[90] Pieremanuele Canepa, Calvin A. Arter, Eliot M. Conwill, Daniel H. Johnson, Brian A. Shoemaker, Karim Z. Soliman, and T. Thonhauser. High-throughput screening of small-molecule adsorption in MOF. *Journal of Materials Chemistry A*, 1(43):13597–13604, 2013.

[91] Andrew M. Walker, Bartolomeo Civalleri, Ben Slater, Caroline Mellot-Draznieks, Furio Corá, Claudio M. Zicovich-Wilson, Guillermo Román-Pérez, José M. Soler, and Julian D. Gale. Flexibility in a metal-organic framework material controlled by weak dispersion forces: the bistability of mil-53(al). *Angewandte Chemie International Edition*, 49:7501–7503, 2010.

[92] Jesper Kleis, Bengt I. Lundqvist, David C. Langreth, and Elsebeth Schröder. Towards a working density-functional theory for polymers: First-principles determination of the polyethylene crystal structure. *Physical Review B*, 76:100201, Sep 2007.

[93] Eleni Ziambaras, Jesper Kleis, Elsebeth Schröder, and Per Hyldgaard. Potassium intercalation in graphite: A van der waals density-functional study. *Physical Review B*, 76:155425, Oct 2007.

[94] Kyuho Lee, Kristian Berland, Mina Yoon, Stig Andersson, Elsebeth Schröder, Per Hyldgaard, and Bengt I. Lundqvist. Benchmarking van der waals density functionals with experimental data: potential-energy curves for h$_2$ molecules on cu(111), (100) and (110) surfaces. *Journal of physics. Condensed matter*, 24:424213, 2012.

[95] Roberta Poloni, Berend Smit, and Jeffrey B. Neaton. Co$_2$ capture by metal-organic frameworks with van der waals density functionals. *The Journal of Physical Chemistry A*, 116(20):4957–4964, 2012.

[96] Svetla D. Chakarova-Käck, Elsebeth Schröder, Bengt I. Lundqvist, and David C. Langreth. Application of van der waals density functional to an extended system: Adsorption of benzene and naphthalene on graphite. *Physical Review Letters*, 96:146107, Apr 2006.

[97] Lingzhu Kong, Valentino R. Cooper, Nour Nijem, Kunhao Li, Jing Li, Yves J. Chabal, and David C. Langreth. Theoretical and experimental analysis of h$_2$ binding in a prototypical metal-organic framework material. *Physical Review B*, 79:081407, Feb 2009.

[98] Wei Zhou, Hui Wu, and Taner Yildirim. Enhanced h$_2$ adsorption in isostructural metal-organic frameworks with open metal sites: Strong dependence of the binding strength on metal ions. *Journal of the American Chemical Society*, 130(46):15268–15269, 2008. PMID: 18950163.

[99] Lingzhu Kong, Yves J. Chabal, and David C. Langreth. First-principles approach to rotational-vibrational frequencies and infrared intensity for h$_2$ adsorbed in nanoporous materials. *Physical Review B*, 83:121402, Mar 2011.

[100] D. C. Langreth, M. Dion, H. Rydberg, E. Schröder, P. Hyldgaard, and B. I. Lundqvist. Van der waals density functional theory with applications. *International Journal of Quantum Chemistry*, 101(5):599–610, 2005.

[101] Elisa Londero and Elsebeth Schröder. Role of van der waals bonding in the layered oxide v$_2$o$_5$: First-principles density-functional calculations. *Phys. Rev. B*, 82:054116, Aug 2010.

[102] Pascal D. C. Dietzel, Rune E. Johnsen, Helmer Fjellvag, Silvia Bordiga, Elena Groppo, Sachina Chavan, and Richard Blom. Adsorption properties and structure of co$_2$ adsorbed on open coordination sites of metal-organic framework ni$_2$(dhtp) from gas adsorption, ir spectroscopy and x-ray diffraction. *Chemical communications*, pages 5125–5127, 2008.

[103] Hui Wu, Jason M. Simmons, Gadipelli Srinivas, Wei Zhou, and Taner Yildirim. Adsorption sites and binding nature of co$_2$ in prototypical metal-organic frameworks: A combined neutron diffraction and first-principles study. *The Journal of Physical Chemistry Letters*, 1:1946–1951,

2010.

[104] L. Valenzano, B. Civalleri, S. Chavan, G. T. Palomino, C. O. Areán, and S. Bordiga. Computational and experimental studies on the adsorption of co , n_2 , and co_2 on mg-mof-74. *The Journal physical chemistry C*, 114:11185–11191, 2010.

[105] Jie Yang, Anna Grzech, Fokko M. Mulder, and Theo J. Dingemans. Methyl modified mof-5: a water stable hydrogen storage material. *Chemical communications*, 47:5244–5246, 2011.

[106] Tianjiao Wu, Lingjuan Shen, Matthew Luebbers, Chunhua Hu, Qingmei Chen, Zheng Ni, and Richard I. Masel. Enhancing the stability of metal-organic frameworks in humid air by incorporating water repellent functional groups. *Chemical communications*, 46:6120–6122, 2010.

[107] Jeffery A. Greathouse and Mark D. Allendorf. The interaction of water with mof-5 simulated by molecular dynamics. *Journal of the American Chemical Society*, 128(33):10678–10679, 2006.

[108] Deyun Ma, Yingwei Li, and Zhong Li. Tuning the moisture stability of metal-organic frameworks by incorporating hydrophobic functional groups at different positions of ligands. *Chemical communications*, 47:7377–7379, 2011.

[109] John J. Low, Annabelle I. Benin, Paulina Jakubczak, Jennifer F. Abrahamian, Syed A. Faheem, and Richard R. Willis. Virtual high throughput screening confirmed experimentally: Porous coordination polymer hydration. *Journal of the American Chemical Society*, 131(43):15834–15842, 2009. PMID: 19810730.

[110] Dipendu Saha and Shuguang Deng. Structural stability of metal organic framework mof-177. *The Journal of Physical Chemistry Letters*, 1(1):73–78, 2010.

[111] Y. F. Chen, J. Y. Lee, R. Babarao, J. Li, and J. W. Jiang. A highly hydrophobic metal-organic framework zn(bdc)(ted)0.5 for adsorption and separation of ch_3oh/h_2o and co_2/ch_4: An integrated experimental and simulation study. *The Journal of Physical Chemistry C*, 114(14):6602–6609, 2010.

[112] Jeong Yong Lee, David H. Olson, L. Pan, Thomas J. Emge, and J. Li. Microporous metal-organic frameworks with high gas sorption and separation capacity. *Advanced Functional Materials*, 17(8):1255–1262, 2007.

[113] Danil N. Dybtsev, Hyungphil Chun, and Kimoon Kim. Rigid and flexible: a highly porous metal-organic framework with unusual guest-dependent dynamic behavior. *Angewandte Chemie International edition*, 43:5033–5036, 2004.

[114] H. Kitagawa. Metal-organic frameworks: Transported into fuel cell. *Nature Chemistry*, 1:689–690, 2009.

[115] Francesc X. Llabrés i Xamena, Avelino Corma, and Hermenegildo Garcia. Applications for metal - organic frameworks (mofs) as quantum dot semiconductors. *Journal of Physical Chemisty C*, 111:80–85, 2007.

[116] Jeff A Hurd, Ramanathan Vaidhyanathan, Venkataraman Thangadurai, Christopher I. Ratcliffe, Igor L. Moudrakovski, and George K. H. Shimizu. Anhydrous proton conduction at 150 °c in a crystalline metal-organic framework. *Nature chemistry*, 1:705–710, 2009.

[117] Shengqian Ma, Xi-Sen Wang, Daqiang Yuan, and Hong-Cai Zhou. A coordinatively linked yb metalorganic framework demonstrates high thermal stability and uncommon gas-adsorption selectivity. *Angewandte Chemie International Edition*, 47(22):4130–4133, 2008.

[118] Daofeng Sun, Shengqian Ma, Yanxiong Ke, Tracy M. Petersen, and Hong-Cai Zhou. Synthesis, characterization, and photoluminescence of isostructural mn, co, and zn mofs having a diamondoid structure with large tetrahedral cages and high thermal stability. *Chemical communications*, pages 2663–2665, 2005.

[119] Chi Yang, Xiaoping Wang, and Mohammad A. Omary. Fluorous metalorganic frameworks for high-density gas adsorption. *Journal of the American Chemical Society*, 129(50):15454–15455, 2007. PMID: 18034494.

[120] Chi Yang, Xiaoping Wang, and Mohammad A. Omary. Crystallographic observation of dynamic gas adsorption sites and thermal expansion in a breathable fluorous metal-organic framework.

Angewandte Chemie International Edition, 48:2500–2505, 2009.

[121] Chi Yang, Ushasree Kaipa, Qian Zhang Mather, Xiaoping Wang, Vladimir Nesterov, Augustin F. Venero, and Mohammad A. Omary. Fluorous metalorganic frameworks with superior adsorption and hydrophobic properties toward oil spill cleanup and hydrocarbon storage. *Journal of the American Chemical Society*, 133(45):18094–18097, 2011.

[122] Brian Kolb and T. Thonhauser. van der waals density functional study of energetic, structural, and vibrational properties of small water clusters and ice i_h. *Physical Review B*, 84(4):045116, July 2011.

[123] Anastasios I. Skoulidas and David S. Sholl. Self-diffusion and transport diffusion of light gases in metal-organic framework materials assessed using molecular dynamics simulations. *The Journal of Physical Chemistry B*, 109(33):15760–15768, 2005.

[124] Emmanuel Haldoupis, Taku Watanabe, Sankar Nair, and David S. Sholl. Quantifying large effects of framework flexibility on diffusion in mofs: Ch_4 and co_2 in zif-8. *ChemPhysChem*, 13(15):3449–3452, 2012.

[125] Qingyuan Yang and Chongli Zhong. Molecular simulation of adsorption and diffusion of hydrogen in metal-organic frameworks. *The Journal of Physical Chemistry B*, 109(24):11862–11864, 2005. PMID: 16852458.

[126] Saeed Amirjalayer, Maxim Tafipolsky, and Rochus Schmid. Molecular dynamics simulation of benzene diffusion in mof-5: Importance of lattice dynamics. *Angewandte Chemie International Edition*, 46(3):463–466, 2007.

[127] Anastasios I. Skoulidas. Molecular dynamics simulations of gas diffusion in metal-organic frameworks: Argon in cubtc. *Journal of the American Chemical Society*, 126(5):1356–1357, 2004. PMID: 14759190.

[128] Emmanuel Haldoupis, Sankar Nair, and David S. Sholl. Efficient calculation of diffusion limitations in metal organic framework materials: A tool for identifying materials for kinetic separations. *Journal of the American Chemical Society*, 132(21):7528–7539, 2010. PMID: 20450176.

[129] Bei Liu, Qingyuan Yang, Chunyu Xue, Chongli Zhong, and Berend Smit. Molecular simulation of hydrogen diffusion in interpenetrated metal-organic frameworks. *Physical chemistry chemical physics*, 10:3244–3249, 2008.

[130] Wendy L. Queen, Craig M. Brown, David K. Britt, Pawel Zajdel, Matthew R. Hudson, and Omar M. Yaghi. Site-specific co_2 adsorption and zero thermal expansion in an anisotropic pore network. *The Journal of Physical Chemistry C*, 115(50):24915–24919, 2011.

[131] Zongbi Bao, Liang Yu, Qilong Ren, Xiuyang Lu, and Shuguang Deng. Adsorption of co_2 and ch_4 on a magnesium-based metal organic framework. *Journal of colloid and interface science*, 353:549–556, 2011.

[132] Amani M. Ebrahim, Benoit Levasseur, and Teresa J. Bandosz. Interactions of no_2 with zr-based mof: Effects of the size of organic linkers on no_2 adsorption at ambient conditions. *Langmuir*, 29(1):168–174, 2013.

[133] Jiamei Yu, Yuguang Ma, and Perla B. Balbuena. Evaluation of the impact of h_2o, o_2, and so_2 on postcombustion co_2 capture in metal-organic frameworks. *Langmuir*, 28(21):8064–8071, 2012.

[134] Kuang Yu and J.R. Schmidt. Comment on "how well do metal-organic frameworks tolerate flue gas impurities?". *The Journal of Physical Chemistry C*, 117(6):3192–3192, 2013.

[135] Lifeng Ding and A. Özgür Yazaydin. How well do metal-organic frameworks tolerate flue gas impurities? *The Journal of Physical Chemistry C*, 116(43):22987–22991, 2012.

[136] Francçois-Xavier Coudert, Caroline Mellot-Draznieks, Alain H. Fuchs, and Anne Boutin. Prediction of breathing and gate-opening transitions upon binary mixture adsorption in metal-organic frameworks. *Journal of the American Chemical Society*, 131(32):11329–11331, 2009. PMID: 19637918.

[137] Canan Gücüyener, Johan van den Bergh, Jorge Gascon, and Freek Kapteijn. Ethane/ethene separation turned on its head: Selective ethane adsorption on the metal-organic framework zif-7

through a gate-opening mechanism. *Journal of the American Chemical Society*, 132(50):17704–17706, 2010.

[138] Marc Pera-Titus and David Farrusseng. Guest-induced gate opening and breathing phenomena in soft porous crystals: Building thermodynamically consistent isotherms. *The Journal of Physical Chemistry C*, 116(2):1638–1649, 2012.